DOI: 10.15587/978-617-8360-05-4.CH2

Oleksij Fomin, Pavlo Prokopenko, Mariia Miroshnykova, Gregori Boyko, Andriy Klymash

CHAPTER 2

STUDY OF SAFETY INDICATORS AND TECHNICAL CONDITION OF ROLLING STOCK BY MOBILE SYSTEMS

ABSTRACT

The organization of the movement of freight trains in Ukraine is an important factor in the integration of the country's railway transport into the European system. Currently, a situation has arisen that requires a significant renewal of the freight car park with modern cars to meet the requirements of freight transportation. Also, a significant drawback of railway transport of Ukraine is the limitation of the speed of trains, which include freight cars with a reduced container in an empty state, therefore, at the moment, the issue of improving the methodological and software and instrumental testing tools for evaluating the quality and safety indicators of the movement of such cars is relevant at the moment.

Subsection 2.1 offers methods and approaches for assessing quality indicators, traffic safety, and the technical condition of cars. The first method of measuring mechanical stresses in the surface layers of elements of load-bearing structures of rolling stock by the method of tensometry. The second method of measuring contact forces: due to the deformation of the discs of the wheels of the wheel pairs.

Subsection 2.2 proposes a method of in-depth processing of the results of road tests of rolling stock is proposed. The essence is to perform a spectral analysis of dynamic processes for various elements of the load-bearing structures of the freight car, with the aim of identifying the relationships between the oscillatory processes of the load-bearing structures and the frequencies at which the interaction between them occurs.

Subsection 2.3 forms and implements the general requirements for the mobile system for determining the quality and safety indicators of the movement of freight cars with reduced containers in operation were formed and implemented. This mobile system allows running tests without involving the laboratory car, which reduces costs and time for conducting such tests by 25.8 %. A method of in-depth processing of the results of road tests of rolling stock is proposed.

Subsection 2.4 formulates the general requirements for the software and hardware complex for determining the dynamic load of running parts under the conditions of operation of rolling stock. Technical solutions have been implemented regarding the means of running tests of rolling stock to determine the dynamic loading of running parts in operating conditions, which increases the effectiveness of forecasted assessments and increases the efficiency of testing.

A set of software subsystems for collecting measurement information, determining movement smoothness and safety indicators of rolling stock according to simplified schemes has been developed.

KEYWORDS

Freight cars, running tests, traffic quality and safety indicators, dynamic processes, stability, mobile system, dynamics, software.

The organization of the movement of freight trains in Ukraine is a key aspect of the integration of the country's railway transport into the European system. Today, there is a need for a significant renewal of the fleet of freight cars with modern models in order to meet the requirements of freight transportation. One of the serious shortcomings of railway transport in Ukraine is the limitation of the speed of movement of trains containing cargo cars with reduced containers in an empty state. This makes the issue of improving methodological and software, as well as instrumental means for tests that evaluate the indicators of the quality and safety of the movement of such cars, urgent. As a result of their unsatisfactory movement dynamics, certain groups of freight cars, such as platform cars, are limited to a speed of up to 60 km/h, which negatively affects the overall speed of freight transportation by rail.

In recent years, rail transport has been rapidly developing and integrated into the high-speed rail system. The safety of train operation is becoming a more acute issue. To assess the safety quality of the movement of cars, locomotives and other types of rail rolling stock, there are various approaches to assessing safety conditions and solving this problem.

In [1], the results of the study and establishment of the mechanism of interaction between a railway wheel and a rail are given. The modeling is based on the fundamental theory of circular motion kinematics. The proposed method makes it possible to determine the characteristic criteria of the kinematics of the interaction of the cross-section of the tire of the wheel pairs of the rolling stock with the lateral sides of the rail heads. However, the work does not describe the process of interaction between the railway wheel and the rail from the point of view of traffic safety.

The paper [2] presents a theoretical basis for modeling the interaction of a railway car and a track, in which the dynamic equations of motion of car-track systems are built by effectively connecting linear and nonlinear dynamic characteristics. The result of this study is the determination of the critical speed of a railway train and the localization of track irregularities through the effective integration of a dynamic modeling model, a probabilistic model of track irregularities and a time-frequency analysis method. But the work does not consider the possibility of developing a mobile system for determining the indicators of the interaction of a railway car and a track based on the conducted research.

The authors of the paper [3] investigate the longitudinal forces acting on a railway car for different loading conditions of the cars in the train. Three different types of cars are considered

in the work, namely fully loaded, partially loaded and empty cars. The purpose of this work is to determine the best place for their location in a freight train where the smallest longitudinal forces occur, regardless of the car loading scheme. However, the work does not assess the influence of horizontal forces on the railway car, which significantly affect the safety of the movement of railway cars.

The article [4] presents a study of the descent of freight cars in symmetric turnouts No. 6. A dynamic model of a semi-car and a model of a flexible turnout that undergoes derailment when the wheel flange is lifted is presented. In addition, a full-scale wheel-rail interaction test was conducted to verify the dynamic model. As a result of the simulation of derailment when lifting, the wheels are consistent with the research data, and the safety of the cart depends on the condition of both the front and rear wheels.

In the article [5], the authors present the concept of a smart railway car modeled from smart components. This concept can meet the safety requirements of a complex railway system. Adding self-diagnostic features to a rail car reduces the risk of accidents. This paper also presents the concept and functional model of this railway car and illustrates the utility of this concept based on investigated railway accidents.

The study [6] describes the behavior of dynamic derailment caused by the failure of rail connections of a railway switch, as well as the assessment of the impact of such parameters on the safety of train operation. The developed model takes into account the transverse difference between the sections of the rail connection, which directly cause the wheel lift. The conducted research indicates that the proposed derailment model is able to effectively assess operational safety as a result of various wheel and track defects, and thus provide a basis for providing a cost-effective platform for future optimization of railway track and rolling stock parameters.

In [7], the authors study the influence of gaps between the blocks, changes in the wheel-rail friction coefficient, and the radius of the track curve on the nonlinear critical speed of a railway vehicle. The effect of the gaps between the axle boxes on the wear of the wheels and the interaction of the wheels with the railway track was also investigated.

The paper [8] describes the dynamic behavior of the wheel-rail interaction under various surface contaminations of the rail track using the methodology of experimental and numerical modeling. The results of the study showed that the wheel-rail creep force drops sharply when the wheel enters the low adhesion zone, and when the adhesion is restored, there is a sudden increase in the creep force, which negatively affects the dynamics of the railway car.

In the study [9], a refined wheel-rail contact formula was proposed for the analysis of nonlinear train-track interaction, which takes into account the geometry of the wheel and rail. While most of the existing methods consider contact forces as external forces, the work uses modeling of the behavior of the contact surface based on Hertz's theory and Kalker's laws. The proposed refined mathematical model is confirmed by experimental data.

In the article [10] three-dimensional numerical modeling of the moving load of the wheel-rail interaction for high-speed and heavy trains is investigated. Simulations were performed in ANSYS

with a hybrid model involving a flexible wheel pair moving on a pair of rigid rails, which helped in estimating the frictional stresses at the wheel-rail interface during train motion. As a result of the work, it was found that contact pressure and frictional stress increase quadratically with increasing train speed.

In the article [11], the authors proposed a three-dimensional (3-D) model of train-track interaction. As a result of the study of the developed dynamic model, it was found that this model demonstrates high computational stability, accuracy and efficiency in comparison with traditional solutions; in addition to some key parameters such as bridge element length, the length of the track and bridge section in numerical integration can be conveniently refined using this model.

In the paper [12], the authors develop a dynamic model for studying the vertical interaction of the rail track and the car system. The developed model is verified using several test data and other numerical models.

In the article [13], the authors present an analysis of the influence of creep paths on the contact forces of the wheel and rail. The simulation results showed that the maximum normal wheel-rail contact stresses are less than 1600 MPa in the range of typical conditions of normal operation.

The article [14] presents the features and results of the cataloging of the supporting system of semi-cars, the application of this approach for the end wall of one of the basic models of cars.

In work [15], the authors describe the problem of various deformations at all stages of operation of freight cars. The main type of these deformations are residual deformations that occur during welding as a result of thermal exposure.

The authors of the article [16] describe the process of conducting control tests of tank cars for dangerous goods. The testing methodology described in this work was used during the research.

In the article [17], the author highlights the results of work on determining ways to increase the degree of ideality of freight cars and forecasting the evolution of the chassis of new generation cars. Review of examples of application of the idealistic strategy of improving the undercarriage of railway universal freight semi-cars.

In [18], the authors describe a method of increasing the efficiency of the braking system by controlling the cooling of the friction surfaces using adaptive air supply; a mathematical model of air pressure supply to the friction contact of the brake was created in order to obtain the optimal diameter of the holes of the friction linings and the speed of air supply.

In work [19], the authors present the features of mathematical modeling of the dynamic load of containers placed on the platform during a maneuvering collision. Numerical values of accelerations acting on the container are determined. The results are confirmed by computer simulation. The developed models are tested according to the F-criterion.

Based on the results of the analysis of literary sources [1–19], it can be concluded that the issue of direct measurement of the forces of interaction of wheel pairs with rails using the measurement of wheel deformations at control points is relevant and requires research.

2.1 METHODS AND APPROACHES FOR EVALUATING INDICATORS OF QUALITY, TRAFFIC SAFETY AND TECHNICAL CONDITION OF CARS

2.1.1 MEASUREMENT OF DEFORMATIONS OF LOAD-BEARING STRUCTURES. GENERAL INFORMATION

To measure the mechanical stresses in the surface layers of the elements of the load-bearing structures of the rolling stock, the methods and means of strain measurement are used, that is, strain gauges and recording equipment. The operation of the strain gauge is based on the tensor effect of the conductor or semiconductor, which is attached to the surface of the supporting element of the structure with a special glue. Thus, deforming together with the metal element when it is loaded, the strain gauge changes its electrical resistance.

Strain gauges are divided into wire, foil and semiconductor tensors by design. The wire strain gauge schematically shown in **Fig. 2.1**, is a wire spiral 1 placed between two layers of thin paper 2. Terminals 3 are soldered to the spiral for connecting strain gauges to each other in an electrical circuit. Constantan (copper and nickel alloy) or nichrome (nickel and chromium alloy) wire is used for strain gauges. The diameter of such a wire is 0.015...0.025 mm.

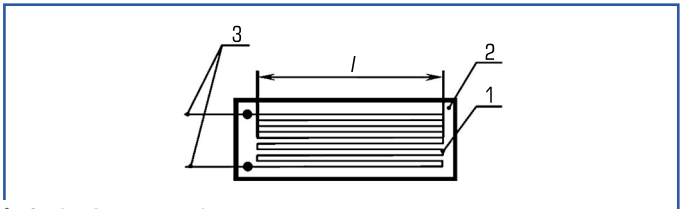

Fig. 2.1 Strain gauge diagram

Foil strain gauges are made by etching or stamping from Constantan foil fixed on a film or paper base. Semiconductor strain gauges are made of semiconductor materials in the form of thin strips of germanium or silicon with soldered metal terminals. Such strain gauges have a sensitivity 1–2 orders of magnitude higher than wire or foil ones.

The main characteristics of strain gauges are nominal resistance R, base l and sensitivity γ. The sensitivity of the strain gauge is defined as the ratio of the relative change in resistance to its relative elongation:

$$\gamma = \frac{\frac{\Delta R}{R}}{\varepsilon}, \qquad (2.1)$$

where ΔR – the change in resistance of the tensor when it is deformed; ε – the relative elongation of the conductor.

The change in resistance of the strain gauge during deformation is very small, usually of the order of several hundreds of Ohms. One of the most convenient means of measuring such changes is the Wheatstone bridge. It includes four resistors connected to a DC power supply, as shown in **Fig. 2.2**.

If $R_1=R_2=R_3=R_4$, this indicates that the bridge is balanced, and the voltmeter connected to the measuring diagonal of the bridge will show 0 V. The principle of operation of the bridge circuit is that the electric current flowing through the resistors in the case unbalanced state of the bridge creates a potential difference in the measuring diagonal, and an electric current will flow through the measuring device.

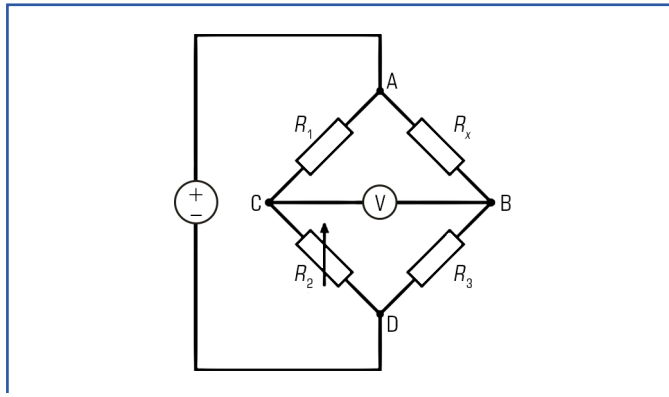

Fig. 2.2 Connection diagram of the Wheatstone bridge with balancing

In order to measure the voltage, the resistors shown in **Fig. 2.2**, are replaced by one or more strain gauges (which are usually variable resistors whose resistance changes with a change in voltage). At the beginning of the test, a balancing potentiometer is used to balance the bridge, setting 0 V on the voltmeter. Applying a test load will change the resistance of the strain gauge and bring the bridge out of balance, producing a voltage proportional to the applied voltage.

The bridge can contain one, two, or four strain gauges according to the schematics, such a configuration is known as one-fourth, half-bridge, and full-bridge, respectively. Of these three schemes, one fourth of the bridge will have the lowest sensitivity. Failure to take precautions can lead to errors because strain gauges are sensitive to thermal effects. In order to prevent this, one of the strain gauges adjacent to the active one can be replaced by a so-called compensation one. This strain gauge is identical to the active one, is in the same ambient conditions, but is not subjected to the load, which is achieved, for example, by installing it on an unstressed part of the object under test. Both strain gauges are subjected to the same temperature changes, and as a result, the effect of any resulting effect on the balance of the bridge due to thermal effects is canceled out.

A half bridge will have a higher sensitivity than a quarter bridge because the additional strain gauge will produce a larger unbalanced voltage across the Wheatstone bridge. The presence of two active strain gauges also excludes any thermal effects as described above. Of the three schemes, the full bridge has the highest sensitivity. In addition, it is self-compensating for temperature changes.

It should be noted that the changes in the output voltage from bridges for measuring mechanical stresses are usually very small and therefore need to be amplified as close to the bridge as possible. Cable lines must be fully enclosed and shielded to prevent distortion of test data.

When measuring the deformation of the surface of the wheel disc, a statistical method was adopted to estimate the measurement error with a probability of $P=0.95$. The deformation ε_i measured by the device under a unit load is determined by the formula:

$$\varepsilon_i = \frac{p \cdot \overline{U}_{out}}{K \cdot U_{sup}}, \tag{2.2}$$

in which

$$\overline{U}_{out} = \frac{1}{n}\sum_{i=1}^{n} U_{i\ out},$$

where $p=2$ – for a half-bridge circuit; U_{sup} – voltage of the measuring system supply, V; $\overline{U}_{out}$ – average value of the output voltage, mV; K – coefficient of tensile sensitivity (1.9–2.04).

The average arithmetic value of deformations is determined by the formula:

$$\overline{\varepsilon} = \frac{\sum_{i=1}^{n}\left(\varepsilon_i\right)}{m}, \tag{2.3}$$

where m – the number of measurement points.

The mean square deviation of the measurement results $\tilde{\sigma}\left(\dot{\Delta}\right)$ is determined by the formula:

$$\tilde{\sigma}\left(\dot{\Delta}\right) = \sqrt{\frac{\sum_{i=1}^{n}\left(\overline{\varepsilon} - \varepsilon_i\right)^2}{m\left(m-1\right)}}. \tag{2.4}$$

The sum of random and non-excluded systematic errors is determined by the formula:

$$\sigma\left(\Delta\right) = \sqrt{\tilde{\sigma}\left(\dot{\Delta}\right)^2 + \tilde{\sigma}_1\left(\Delta_s\right)^2 + \tilde{\sigma}_2\left(\Delta_s\right)^2}, \tag{2.5}$$

where $\tilde{\sigma}_1\left(\Delta_s\right)$ – non-excluded remainder of the systematic error caused by the error of the measuring system; $\tilde{\sigma}_2\left(\Delta_s\right)$ – non-excluded remainder of the systematic error due to the error of the strain gauges.

The upper $\tilde{\Delta}_h$ and lower $\tilde{\Delta}_l$ limits of the measurement error are determined by the formula:

$$\tilde{\Delta}_h = \tilde{\Delta}_l = t_p \sigma(\Delta), \tag{2.6}$$

where t_p – the Student coefficient, which depends on the number of measurements and the given probability [20, 21].

2.1.2 MEASUREMENT OF FORCES BY LOCAL DEFORMATIONS OF CART FRAMES

Strain gauge bridges are widely used when conducting static strength and dynamic running tests of rolling stock. For example, the method of determining vertical and horizontal transverse (frame) forces acting on wheel pairs, according to the rules that are currently in force on railways with a gauge of 1520 mm, involves the measurement of deformations of cart frames.

Strain gauges are pasted on the outer and inner sides of the side frames and assembled into schemes that, as a rule, have good sensitivity with sufficient compensation for temperature deformations. This method allows to continuously measure horizontal (frame) and vertical forces when moving along a track section of any length.

The characteristics of the force action measured in this way in the "cart frame – wheelset" system are calculated using the calculation method to estimate the forces of interaction between the wheels and the rails, the ratio of which determines the so-called reserve coefficient of stability of the wheel from leaving the rail [22–24].

2.1.3 MEASUREMENT OF FORCES OF DIRECT INTERACTION OF WHEELS WITH RAILS

One of the important aspects in the system of direct measurement of the forces of the contact interaction between wheels and rails is the determination of the zones of deformation sensitivity on the wheel disks from the action of vertical and lateral forces. From the determined zones, it is important to localize those in which the deformations were the result of the action of forces in one direction.

To carry out calculations of the stress-strain state of the wheel pair using the finite element method, 3D models of individual elements of the wheel pair and P65 type rails were created in the SolidWorks software package, from which a general 3D model of the wheel pair installed on the rails was created.

To determine these zones, a finite element calculation was performed for three calculation schemes:

a) vertical load of the wheel pair;

b) loading by vertical forces and forces from the action of the tare system;

c) loading of the wheel pair by vertical and horizontal forces when passing curved sections of the track.

Below are the results of the characteristic calculations for the specified load patterns of the wheel pair.

Vertical load. Based on the task of the research, in order to ensure greater visibility of the results, the maximum value in the chart legend was reduced to 10 MPa, since these are the stresses that occur on the wheel disc.

Fig. 2.3 shows a picture of the distribution of calculated stresses in the elements of a wheel pair under the action of a vertical load. As can be seen, the greatest stresses occur in the wheel disc at the point of transition of the disc to the hub part of the wheel and amount to 7.78 MPa, as well as in the hub transition between the neck and the hub part – 46 MPa.

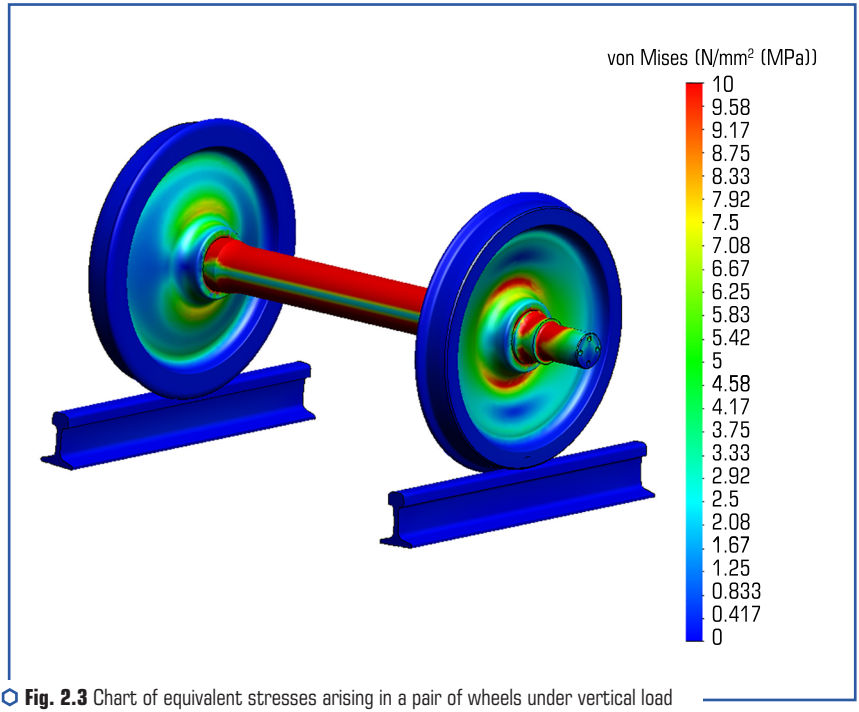

Fig. 2.3 Chart of equivalent stresses arising in a pair of wheels under vertical load

In the axis of the wheelset, which mainly works in bending, the stresses in the cross sections are unevenly distributed, reaching the largest values in the outer fibers and the smallest in the inner fibers, as shown in **Fig. 2.4**.

Fig. 2.5 presents a chart of equivalent stresses, from which it can be seen that when simulating the action of the tare device, the greatest stresses occur in the places between the hub part and the disk and amount to 10.49 MPa.

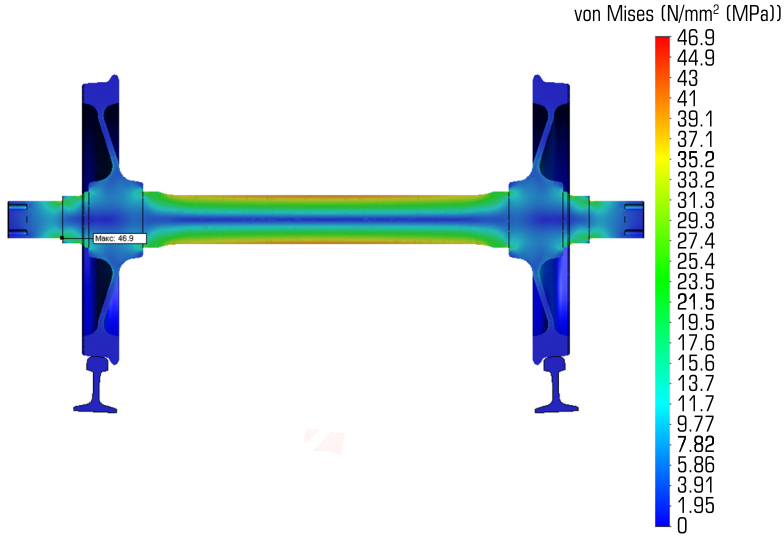

Fig. 2.4 The chart of equivalent stresses arising in a pair of wheels (in cross-section)

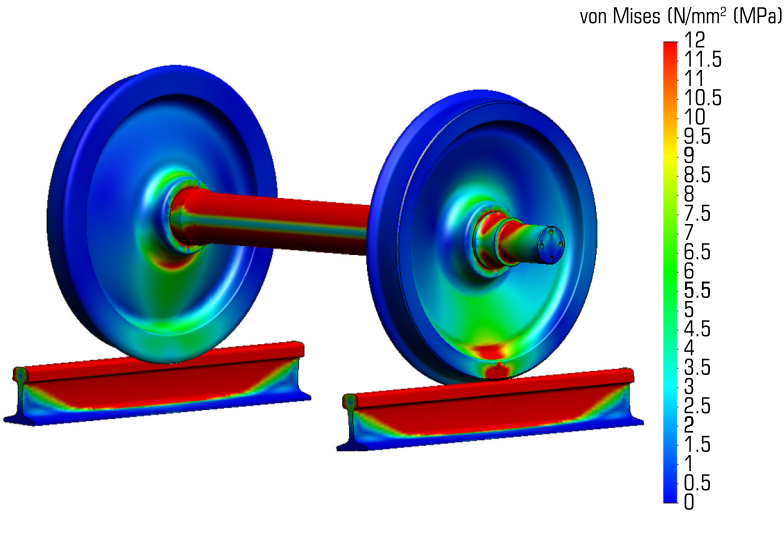

Fig. 2.5 The chart of equivalent stresses arising in a pair of wheels when loaded with a tare device

Fig. 2.6 presents a chart of equivalent stresses, from which it can be seen that when simulating the action of a lateral load, the greatest stresses occur in the places between the hub part and the disk and are equal to 12 MPa.

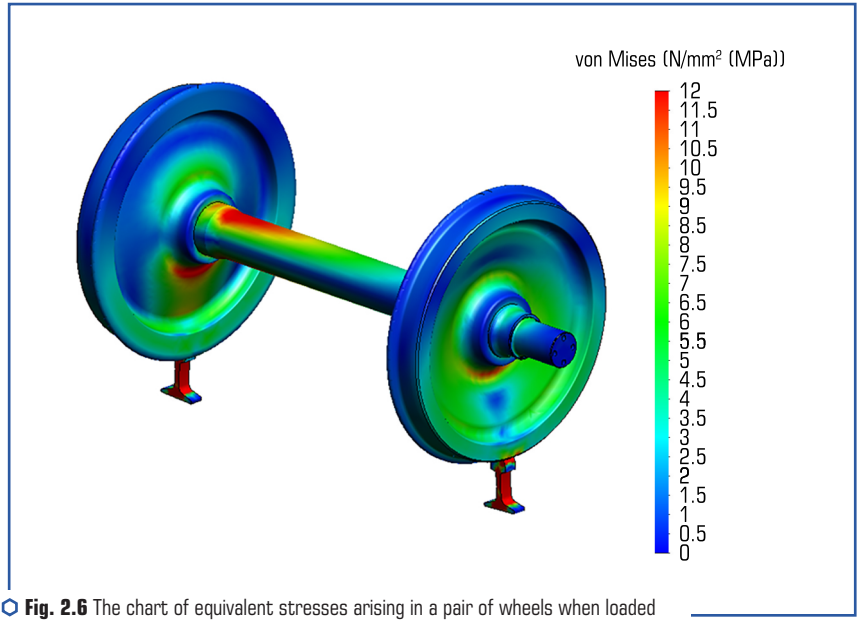

Fig. 2.6 The chart of equivalent stresses arising in a pair of wheels when loaded with vertical and lateral loads

Thus, the most sensitive zone is the zone of the wheel disc at the point of transition of the disc to the hub part of the wheel, but it is also the most sensitive to vertical load. Therefore, to measure the lateral load, it is possible to choose the zone between the hub part and the disk, which is practically sensitive only to lateral forces, and to measure the vertical load, choose the zone in the zone of the rim of the wheel disk [25].

Places of strain gauges on the disc of a wheel pair and methods of their inclusion in the measuring scheme should be such that, with sufficient sensitivity of the scheme to the measured force, influence on the scheme of the force of the other direction is excluded.

Thus, for separate registration of the forces acting on the wheel pair, it is necessary to determine the places of the strain gauges, each of which is sensitive only to the force acting in one direction.

To determine the sensitive zones of action of the vertical and lateral load on the wheel, a diagram of the arrangement of strain gauges (**Fig. 2.7**) and the coordinates of the location of the strain gauges on the wheel of the measuring wheelset was developed. The distance between strain gauges sensitive only to horizontal or only to vertical forces is approximately 55 mm [26].

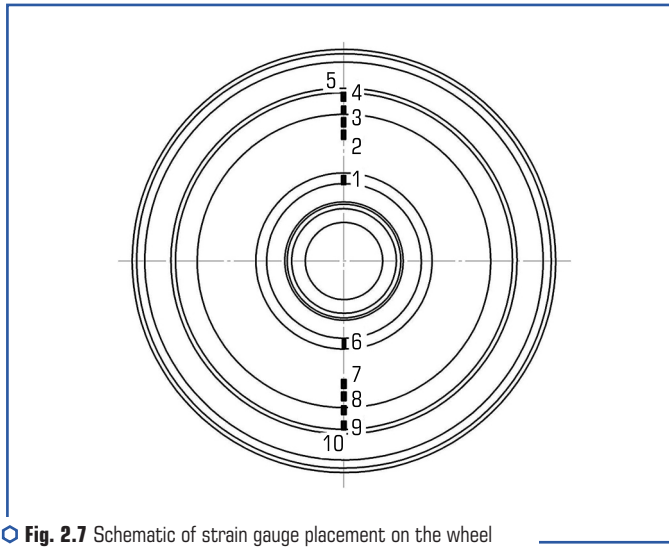

Fig. 2.7 Schematic of strain gauge placement on the wheel of the measuring wheelset

2.1.4 MEASUREMENT OF DYNAMIC INDICATORS OF ROLLING STOCK

In order to measure and evaluate the dynamic load of the crew part of the rolling stock, UM-type low-frequency experimental accelerometer was developed. In order to use this accelerometer for measuring accelerations on rolling stock, a cubic body was developed. The choice of this design of the accelerometer body is determined by its ease of use. It consists of a case, a cover, a circuit board and an electrical connector, as well as fasteners (magnet, bolts, washers, nuts).

The case has a cut-out in which the board with the ADXL 278 microcircuit is placed on one side and the electrical connector is installed on the other. The cover and the electrical connector are filled with epoxy glue. The general view of the accelerometer is shown in **Fig. 2.8**.

The measured accelerations can be used as indicators of the quality of the track geometry and to detect local geometric deviations affecting the dynamic behavior of the rolling stock. These measurements should be used in conjunction with basic parameter measurements.

Measurement of accelerations should be carried out in specified places on the body and carts, depending on the need for a specific assessment. Thus, the vertical accelerations of the boxes are measured to detect defects on the rail surfaces and isolated geometric irregularities. Transverse accelerations of the cart are measured to detect short-wave irregularities. According to the lateral and vertical accelerations of the body, track defects affecting the dynamics of the rolling stock are revealed.

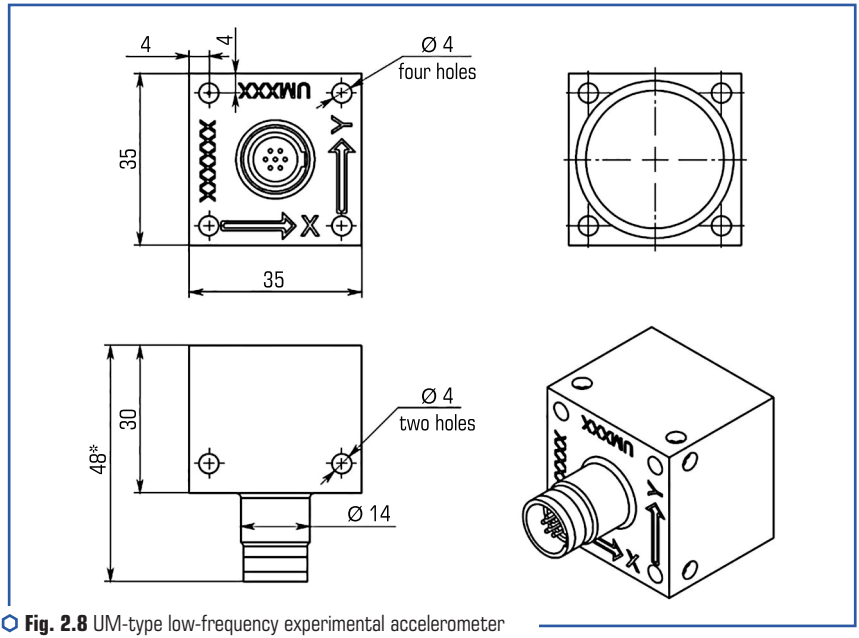

Fig. 2.8 UM-type low-frequency experimental accelerometer

The sampling frequency should be at least 2.5 times higher than the cutoff frequency applied to the signal. Measurements of the accelerations of the carts and the body should be performed in the working range of movement speeds for the line within the tolerance of ±10 %.

In order to measure displacements and evaluate dynamic qualities, cable displacement sensors are used. Cable sensors measure linear displacement using a steel cable that is connected to a sensing element that converts the cable's displacement into a linear output signal [27, 28].

2.2 IMPROVEMENT OF MEANS AND APPROACHES FOR ASSESSING SAFETY INDICATORS AND TECHNICAL CONDITION OF FREIGHT CARS

2.2.1 MATHEMATICAL SUPPORT FOR DETERMINING SAFETY INDICATORS AND TECHNICAL CONDITION OF FREIGHT CARS

The software for evaluating the received experimental data of movement quality indicators was developed in the LabView software shell.

The LabView software system implements the process of in-depth processing of the results of running dynamic tests to identify relationships between the vibrational processes of load-bearing

structures, estimate the frequencies at which the interaction between them occurs and the levels of interaction.

The above-mentioned processing of the test results consists in performing a correlation and spectral analysis of the processes investigated for various elements of the load-bearing structures. The values measured during the tests are compiled into a multidimensional time series $X(t) = \left[x_1(t) / x_p(t) \right]$, in which each line $X_p(t) = \left[x_{p1} \ldots x_{pn} \ldots x_{pN} \right]$ is a one-dimensional series one measuring channel.

Fig. 3.1, *a*, *b* shows the block diagram of the developed software for evaluating the received experimental data of traffic quality indicators and consists of 5 main blocks.

In block 1, the input parameters for processing the results are specified and the location of the resulting file creation is specified.

In block 2, primary data of binary form is read from primary files. Data conversion from binary to text and numeric.

In block 3, the array of data used in further work is defined (so many values of strain gauges, accelerometers, GPS are obtained). The number of received GPS values is determined in relation to the number of values received from tensors and accelerometers, an array of values is formed that come to one GPS value.

In block 4, the array of data is filled that meets the previous requirements for processing in block 1: speed ranges, the number of values per range, etc.

In block 5, the resulting file based on the accumulated array of data in block 4 is written in text form and represents an oscillogram (**Fig. 2.9**).

Next, the resulting file must be filtered with a linear digital filter.

A specialized software module in the LABVIEW software shell is used to estimate the smoothness index of rolling stock.

The software module is a finished application, the input data of which are the digitized oscillograms received from the acceleration sensors and registered by the software hardware recorder based on the programmable controller after initial processing.

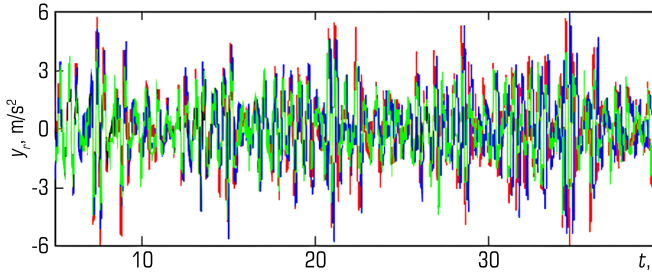

Fig. 2.9 An example of an oscillogram of the resulting file from the measurement of the cart accelerations

The result is the smoothness index value W for the input registration.

The algorithm of the application is as follows.

The size of the input block for calculations is determined. The size of the input block is determined by the base number.

Using the built-in function of LABVIEW, the Fourier transform is performed to construct the power spectrum.

On the basis of the Fourier transformation, frequency arrays and a data array are built in a given frequency range from 0.5 Hz to 20 Hz.

The values of the normalized amplitude-frequency characteristic of the correction filter $q_n(f)$ are calculated according to the formula:

$$q_n(f) = 1.15f \sqrt{\frac{(1+0.1f^2)}{(1+4.04f^2)\left((1+0.0364f^2)^2+0.045f\right)}}. \quad (2.7)$$

The final smoothness index W_j for the input array is calculated according to the formula [29]:

$$W_j = \alpha \cdot \tilde{a}_{kJ}^{0.3}, \quad (2.8)$$

where $\tilde{a}_{kJ}^{0.3}$ – the mean square value of vibration accelerations at the output of the correcting filter, m/s^2; α=4.346 for vertical oscillations [29]; α=4.676 for horizontal (transverse) oscillations [29].

The Butterworth digital filter function of the LABVIEW software shell is used to evaluate safety indicators and quality of rolling stock movement.

The transfer function of the Butterworth filter is given below:

$$K(\omega) = \frac{1}{\sqrt{1+\left(\frac{\omega}{\omega_0}\right)^{2n}}}, \quad (1.9)$$

where ω_0 – the cutoff frequency (it is 1 rad/s); n – the filter order.

The transmission coefficient at 0 is often 1, at the cutoff frequency, regardless of the order of the filter, it is $1/\sqrt{2} = 3$ dB. At ω, which approaches ∞, the amplitude-frequency characteristic approaches zero. The amplitude-frequency characteristic of the Butterworth filter is maximally flat at ω=0 and ω=∞. In general, the amplitude-frequency characteristic decreases from 1 to 0 when the frequency changes from 0 to ∞ (**Fig. 2.10**) [30–32].

Fig. 2.11 shows the results of filtering a signal using a Butterworth filter, obtained from an accelerometer located on the shouldered part of a car that was moving at a speed of 70 km/h.

Filtering the recorded accelerometer signal with a Butterworth filter provides a filtered signal that is used for the movement smoothness metric.

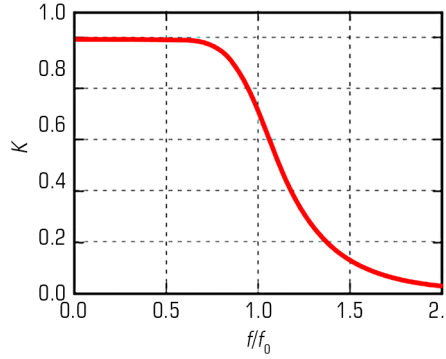

Fig. 2.10 Characteristics of the Butterworth filter

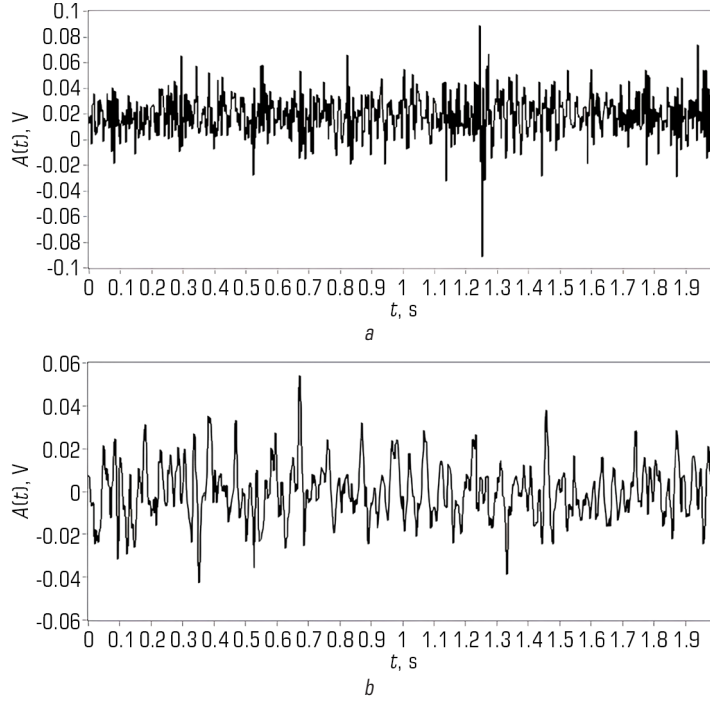

Fig. 2.11 Example of filter operation: *a* – before filtering; *b* – after filtering

2.2.2 SOFTWARE FOR COLLECTING AND REGISTERING SAFETY INDICATORS AND TECHNICAL CONDITION OF CARS

The software of the data collection and registration system performs registration, storage and visualization of changes in information channels (accelerometers, strain gauges). GPS module readings are used to analyze the influence of movement speed on the change of research parameters.

Fig. 2.12 shows a block diagram of the system for collecting and registering measured parameters.

A chassis for 8 modules with a built-in programmable logic device (PLD) and two universal 9205 ADC modules with a maximum sampling frequency of 250 kHz and five 9237 strain gauge modules with a maximum frequency of 50 kHz per channel, a GPS signal receiver module.

Thanks to the built-in PLD, CompactRIO has the ability to implement measurement data processing algorithms at the hardware level with a deterministic execution time of 25 ns without transferring the load to the central processor of the controller. A typical CompactRIO setup includes a controller with a PharLab or VxWorks real-time operating system, a chassis, and I/O modules. The chassis carries the PLD core, is directly connected to universal or specialized input-output modules that have built-in means of matching and processing information signals. There are different chassis models that have different numbers of module slots and differ in the characteristics of the PLD chips.

The developed collection subsystem ensures the operation of the CompactRIO controller.

Thanks to its autonomy, hardware and mass-dimensional characteristics, as well as the ability to work in adverse conditions, CompactRIO can be used to solve a wide range of tasks related to the collection of measurement information and process management.

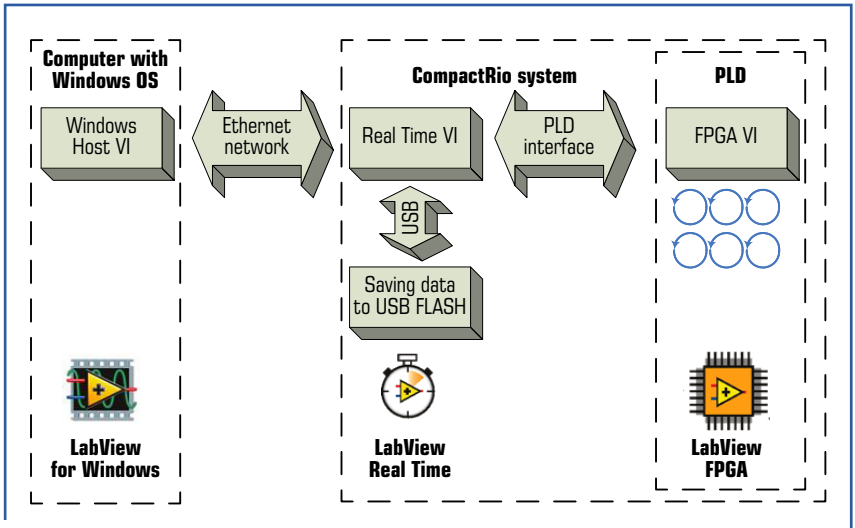

Fig. 2.12 General scheme of the system of collection and registration of measured parameters

Most of the software for CompactRIO is developed according to a scheme that provides for its conditional separation into three levels: a virtual instrument HOST VI on a control PC with a Windows OS, an RT VI on a controller with a real-time OS, and an FPGA VI on a PLD that does not have its own OS, since the logic of the program was implemented directly at the hardware level. Each of the presented levels has its own specific functionality and implements individual functions of the system as a whole.

Typical tasks performed using the HOST VI on a Windows computer are:

– saving data on a computer and accessing databases;
– integration with external information systems;
– organization of the interface.

Typical tasks performed in RT VI on a real-time controller:

– data processing;
– management;
– saving data in the built-in memory of the controller and on external media.

Typical tasks performed in FPGA VI on PLD:

– input-output operations;
– hardware interpretation and management of the process of interaction with the equipment;
– low-level processing of measurement signals.

PLD is a microcircuit whose functionality is determined by programming or "configuration", which is the more common term when working with this class of integrated circuits. The LabView FPGA Module package is an addition to the LabView software environment, which allows to specify the logic operations of the PLD in the form of a regular virtual device instead of programming it using a specialized VHDL language. This package allows to create programs with synchronous and asynchronous parallel loops that are executed at the hardware level and provides time-deterministic data collection and analysis.

The LabVIEW FPGA Module software package completely takes over the multi-step process of converting a virtual device into binary PLD code. At the first stage, the virtual device is converted into text code in VHDL language, which is then compiled by the standard Xilinx ISE industrial compiler into binary form. During the compilation process, the code is optimized according to the speed of execution and the number of logic gates involved.

The result of compilation is a binary file (bitstream file), which completely defines the PLD configuration. When the program starts, the binary file is loaded on the chassis, that is, the PLD configuration process takes place. The binary file can be written to the built-in flash memory and automatically loaded when the system is turned on. When the power is turned off, the configuration is not saved, so the binary must be downloaded again after a power-up. With the appropriate configuration, it can be loaded automatically from the flash memory of the PLD device or by the program, using the controller.

FPGA VI virtual instruments can run completely independently of other system components and remain functional even when the controller fails. Moreover, a buffer can be organized on the PLD, which prevents data loss in a similar situation.

PLD is primarily intended for interpretation, synchronization, control, data collection and preliminary digital processing of information signals, control of each input-output module.

A virtual device for a CompactRIO controller usually includes two or more loops: a loop with critical priority, in which the control and data processing algorithms are implemented, and a loop with normal priority, which is responsible for saving data, a remote web interface, and communication over an Ethernet network or RS-232 bus.

To raise the data received from the modules to the level of the real-time controller, the CompactRIO platform provides three ways: through the elements of the front panel, using the mechanism known in LabView as local variables (Local Variables), and through the DMA FIFO buffer. The first two approaches are relatively simple from the point of view of implementation, but suboptimal from the point of view of efficiency. At the same time, the DMA FIFO method allows to receive data obtained at high sampling rates from a large number of modules without delay. One of the advantages of DMA mode is that data transfer occurs independently of the central processor.

PLD devices that support DMA FIFO buffers have direct access to memory, unlike other methods that require the mandatory participation of the processor. Direct memory access is implemented by capturing the PCI bus (bus mastering) by the PLD device, in which it gets access to bus management, and therefore, access to memory, bypassing the processor.

The DMA FIFO buffer consists of two parts: one part is in the PLD memory, the other part is in the memory of the controller. PLD can be written to or read from the buffer element by element using the FIFO Read and FIFO Write methods, and the controller can be written to or read from samples of elements. Communication between the two parts of the buffer is carried out using the software-hardware DMA controller. Thus, from a software perspective, look like a single FIFO buffer.

The virtual device FPGA VI on the PLD implements the functionality of initialization, clocking, polling of data collection modules and subsequent loading of the received readings into the DMA FIFO buffer. To ensure a deterministic sequence of command execution, the structure of the programming language in LabView "Flat Sequence Structure" is used, in which the elements of polling modules and writing to the buffer are located.

The DMA FIFO buffer is polled cyclically at a time interval set by a timer at the real-time controller level, after which the readings obtained as integers according to the dynamic range and bit rate of the acquisition module are normalized by the values of accelerations and deformations. The received data is sent to a virtual device, which ensures their processing and storage on an external drive connected via a USB bus.

CompactRIO controllers have a built-in USB 2.0 controller, but not all storage devices support this standard, which can lead to significant recording delays, which, in turn, lead to overflow of the DMA FIFO buffer and incorrect operation of the system as a whole.

In the presented system, there is no virtual control device placed on a personal computer, and the LabView Remote Panel mechanism is used instead. This function implements the so-called Client-Server model, where the server is the controller, and the client is any computer with LabView installed. By default, CompactRIO is licensed for one external connection, but the number can

be expanded. To activate the Remote Panel on the controller, it is necessary to activate the Web server in the project settings and select those virtual devices to which remote access must be allowed. This function allows to significantly reduce the time required for the development of HOST VI, but it can create a load on the data transmission network.

In addition to the collection modules, for time synchronization and acquisition of current speed and coordinates, a GPS receiver is also connected to the controller, which is installed on the chassis in the same way as standard modules. Because the receiver is manufactured by a third-party company, the LabView Real Time Module does not have a standard means of acquiring GPS data, so it uses a set of closed virtual devices that are installed separately to interact with it. In addition, to ensure the correct functioning of the module as part of the project, it is also possible to add the SubVIs supplied with the module to the FPGA VI. If the initialization is successful, the GPS data is presented as a cluster or directly in a text format that can be used to debug the software or perform other tasks [33].

Therefore, the proposed scheme of the system for collecting and registering measured parameters registers the following indicators: vertical and horizontal transverse accelerations of the cart frames and the car body, dynamic stresses in the body and cart frames at different driving modes. In the future, the registered parameters are used to determine the safety indicators and the technical condition of the cars, namely: stress in the structural elements, indicators of vertical and horizontal dynamics, the coefficient of stability of the wheel from derailment, frame forces and acceleration of the body.

2.3 PRACTICAL ASPECTS OF THE IMPLEMENTATION OF IMPROVED MEANS AND APPROACHES FOR DETERMINING AND EVALUATING SAFETY INDICATORS AND THE TECHNICAL CONDITION OF CARS

2.3.1 MOBILE SYSTEM FOR DETERMINING SAFETY INDICATORS AND TECHNICAL CONDITION IN OPERATING CONDITIONS

Operation of rolling stock and complex technical hardware and software systems are usually subject to failures. The reasons for such failures can be: non-compliance with the manufacturing technology, difficult conditions of use, non-compliance with the requirements for the operation of such systems and rolling stock, aging and wear of nodes. Therefore, the implementation of periodic tests and diagnostics of rolling stock during their life cycle on the railways of Ukraine is an urgent and important task.

Currently, the development of measuring equipment and systems provides an opportunity for the implementation of advanced instrumental approaches for evaluating the quality and safety indicators of train traffic and taking measures to prevent emergency situations. The successful experience of implementing diagnostic systems for locomotives and passenger cars substantiates the feasibility of further improvement of methods and means of experimental evaluation of dynamic qualities and indicators of traffic quality and safety during the entire period of rolling stock operation.

The mobile system for determining the quality and safety indicators of the movement of rolling stock in operation should include: sensors primary converters; GPS receiver; cables for signal transmission; system of collection and registration of measurement indicators; transfer of data about the location and status of the system to the server; determination and assessment of traffic quality and safety indicators in the express processing mode.

Sensors are primary transducers – strain gauges and accelerometers. Cables are intended for connecting sensors with recording devices, the working voltage of which is ±10 V. The cables are shielded 6-core, resistant to the influence of external factors with an operating temperature from –40 to +80 °C.

The mobile system should provide autonomous dynamic testing of the rolling stock to determine the coefficient of stability of the wheel from derailment, vertical and lateral forces and acceleration of sprung and non-sprung parts of the rolling stock, as a basis for assessing the quality of scheduled repairs and determining traffic quality and safety indicators in operating conditions.

During running dynamic tests, the following indicators are recorded: vertical and horizontal transverse accelerations of the cart frames and the car body, dynamic stresses in the body and cart frames at different driving modes [34].

2.3.2 HARDWARE AND PRIMARY CONVERTERS OF THE MOBILE SYSTEM

The mobile system for running dynamic tests and evaluation of movement quality and safety indicators based on National Instruments CompactRIO solves a wide range of tasks aimed at monitoring the technical condition of rolling stock during tests and in normal operation.

Strain gauges are connected to the strain gauge module NI 9237 (**Fig. 2.13**), and accelerometers are connected to the ADC module NI 9205 (**Fig. 2.14**), they perform scaling of the instantaneous values of the input voltage and analog-digital conversion into a digital code.

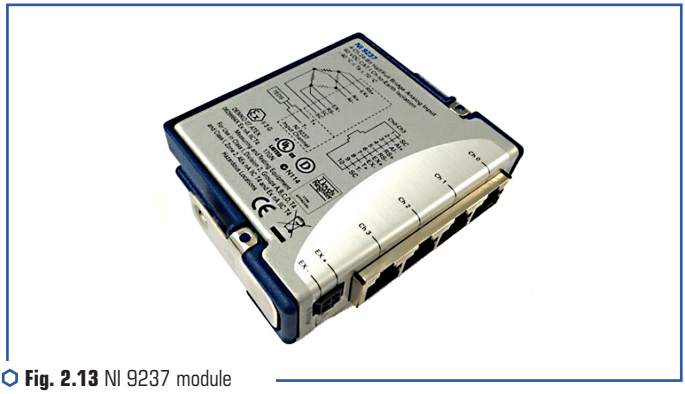

Fig. 2.13 NI 9237 module

Fig. 2.14 NI 9205 module

Digital signals via the internal bus are transmitted from the NI 9237 and NI 9205 modules to the NI 9012 controller (**Fig. 2.15**), from the output of which they are sent to the computer via the Ethernet interface bus, where the measurement information is processed, displayed and stored.

Fig. 2.15 NI 9012 controller

The software performs the functions of managing the recording process, initial setting of the mode of registration of signals from measurement channels, modes of operation of the automatic

recorder, mathematical functions of processing, presentation and storage of measurement information. It consists of the following blocks:

– software for flashing programmable logic;
– integrated microcircuit (PLD) located in the NI 9104 chassis (**Fig. 2.16**);
– application software of the NI 9012 controller;
– client part of the application software of the registrar of the host computer.

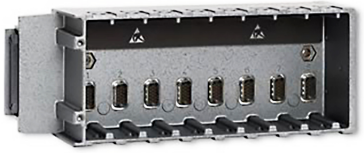

Fig. 2.16 NI 9104 chassis

The software of the software-hardware logger is developed in the LabView FPGA software shell.

The application software is designed to read measurement data from channels selected by the user at the hardware level with a given sampling frequency, select the type of connection of the outputs of the primary measuring transducers, and set the voltage measurement limits.

The NI 9012 controller application software consists of two parts. The first part reads data from NI 9237 and NI 9205 ADC modules, performs data processing and writes to the non-volatile memory of the controller. The second part transmits data using the Transmission Control Protocol (TCP) to an external computer.

The computer software, through the user interface, performs general control functions and displays the current measurements on the monitor screen.

The mobile system can work in two functional modes: assessment of quality indicators, traffic safety and strength indicators in real time (**Fig. 2.17**) and measurement of acceleration and deformation in autonomous mode on rolling stock with further processing (**Fig. 2.18**). During the processing of the obtained values, the data obtained with the help of a GPS receiver are used to assess the impact of the change in the speed of movement on the controlled parameters.

The general block diagram of the mobile diagnostic system is shown in **Fig. 2.19**.

Low-frequency accelerometers of the UM type are used to measure and evaluate dynamic indicators of rolling stock. It consists of a shock-resistant and waterproof case, a board with an ADXL 278 microcircuit, a detachable UZNTS 05-7/12VP11 and fastening elements. The general view of the accelerometer is shown in **Fig. 2.20**.

The resulting vibration accelerations can be used to evaluate track quality indicators to identify point geometric deviations that affect the indicators of rolling stock movement dynamics. Measurement data must be used with GPS data and basic measurement parameters.

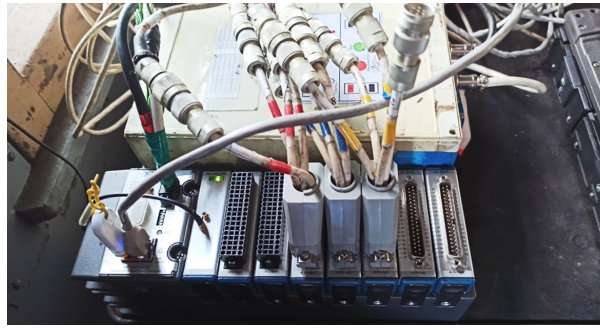

Fig. 2.17 Real-time mobile system

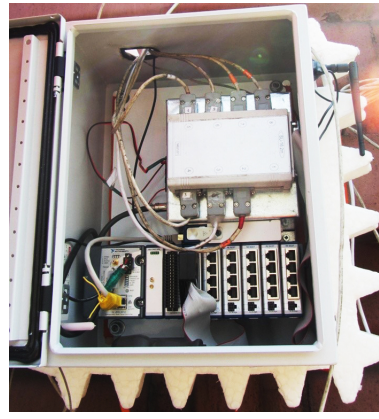

Fig. 2.18 Autonomous mobile system

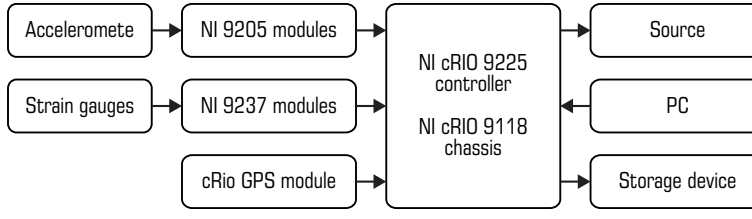

Fig. 2.19 Block diagram of the mobile system

Fig. 2.20 UM-type accelerometer

Vibration acceleration must be measured in certain places of the body and cart, the places are chosen depending on which indicator needs to be evaluated. Vertical accelerations on the axles are measured to evaluate the surface roughness of the track. Transverse accelerations of the cart are measured to evaluate track deviations in the form of short waves. Measurement of transverse and vertical accelerations of the body makes it possible to evaluate dynamic indicators of the quality of movement of rolling stock. The speed at which acceleration measurements of bodies and carts are carried out must be carried out in the established working range.

The measured accelerations can be used as indicators of the quality of the track geometry and to detect local geometric deviations affecting the dynamic behavior of the rolling stock. These measurements should be used in conjunction with basic parameter measurements.

Measurement of accelerations should be carried out in specified places on the body and carts, depending on the need for a specific assessment. Thus, the vertical accelerations of the boxes are measured to detect defects on the rail surfaces and isolated geometric irregularities. Transverse accelerations of the cart are used to detect irregularities with short waves. According to the lateral and vertical accelerations of the body, track defects affecting the dynamic performance of the rolling stock are revealed.

The sampling frequency should be at least 2.5 times higher than the cutoff frequency applied to the signal. Measurements of the accelerations of the carts and the body should be performed in the working speed range for the line within the tolerance of ±10 % [35, 36].

2.3.3 SOFTWARE FOR COLLECTING AND RECORDING MEASUREMENTS

The measurement information collection subsystem collects, stores, and visualizes changes in the information signals of displacement sensors, vibration accelerations, and mechanical deformations.

In addition, data from the GPS receiver is used to analyze the influence of movement speed on changes in controlled parameters, receive accurate time signals, and determine current coordinates. The developed acquisition subsystem provides the operation of a CompactRIO controller with a chassis of 8 modules with a built-in programmable logic devices (PLD) and two universal 9205 ADC modules with a maximum sampling frequency of 250 kHz and five 9237 strain gauge modules with a maximum frequency of 50 kHz per channel, module – GPS signal receiver.

Thanks to the built-in PLD, CompactRIO has the ability to implement measurement data processing algorithms at the hardware level with a deterministic execution time of 25 ns without transferring the load to the central processor of the controller. A typical CompactRIO setup includes a controller with a PharLab or VxWorks real-time operating system, a chassis, and I/O modules. The chassis carries the PLD core, is directly connected to universal or specialized input-output modules that have built-in means of matching and processing information signals. There are different chassis models that have different numbers of module slots and differ in the characteristics of the PLD chips.

Thanks to its autonomy, hardware and mass-dimensional characteristics, as well as the ability to work in adverse conditions, CompactRIO can be used to solve a wide range of tasks related to the collection of measurement information and process management.

Most of the software for CompactRIO is developed according to a scheme that provides for its conditional separation into three levels: a virtual instrument HOST VI on a control PC with a Windows OS, an RT VI on a controller with a real-time OS, and an FPGA VI on a PLD that does not have its own OS, since the logic of the program was implemented directly at the hardware level. Each of the presented levels has its own specific functionality and implements individual functions of the system as a whole.

2.3.4 PRACTICAL STUDIES OF INDICATORS OF THE QUALITY AND SAFETY OF THE MOVEMENT OF FREIGHT CARS IN AN EMPTY STATE AS PART OF A TRAIN

The objects of research were a universal model platform car, a tank car and a hopper car for cement with the roof removed in an empty state.

The mass of the platform car is 20.4 tons, the mass of the hopper car is 22.15 tons, and the mass of the cement hopper car with the roof removed is 18.15 tons.

Tests as part of the train were carried out in 3 options:

– option 1 locomotive – 6 empty semi-cars – experimental coupling – 30 loaded semi-cars;

– option 2 locomotive – 15 loaded semi-cars – experimental coupling – 6 empty semi-cars – 15 loaded semi-cars;

– option 3 – locomotive – 30 loaded semi-cars – experimental coupling – 6 empty semi-cars.

Registration of processes was carried out with the use of strain gauges, which were installed on the structural elements of the carts.

To determine the longitudinal forces acting on the tested car, a coupling dynamometer was used, equipped with strain gauges and a pre-calibrated static load on the stand with a force of up to 3.5 MN.

After installing the measuring equipment on the test cars, the carts were calibrated against vertical and horizontal forces.

To register readings of strain gauges and vibration transducers, a software-hardware complex is used, which consists of a cRIO NI 9012 controller with NI 9237 ADC strain gauge modules, NI 9205 ADC modules and specialized software developed in the LabVIEW software package.

Data processing under static loads was performed using automated experimental data processing complexes.

The results of running dynamic tests were determined on the basis of data (measurements, calculations, control, visual inspection) recorded during the measurements (**Table 2.1**).

Table 2.1 Results of running dynamic tests in an empty state

Car	Permissible value of the stability margin factor	The actual value of the stability margin factor at speed				
		40±5 km/h	50±5 km/h	60±5 km/h	70±5 km/h	80±5 km/h
Platform car	At least 1.3	1.46	1.41	1.31	1.29	1.24
Tank car		1.5	1.47	1.38	1.35	1.33
Hopper car		1.48	1.45	1.38	1.32	1.3

The stability of the wheel from the wheel coming off the rail was determined for the most dangerous cases of a combination of a large transverse force of the interaction of the oncoming wheel with the rail and a small vertical load on this wheel. With the simultaneous action of such a combination of extreme forces over a period of time, it is possible for the crest of the approaching wheel to roll onto the head of the rail and further departure of the car from the rail.

2.4 MOBILE SYSTEM FOR DETERMINING THE DYNAMIC LOAD OF ROLLING STOCK UNDER OPERATING CONDITIONS

2.4.1 GENERAL REQUIREMENTS FOR SOFTWARE AND HARDWARE COMPLEX

A mobile system for determining the dynamic load of running parts of rolling stock in operation should consist of primary converters, a global positioning system receiver, analog signal transmission lines, measuring information collection subsystems, determination of movement safety indicators in the express processing mode, determination of the level of movement smoothness, determination of dynamic tensions.

The primary transducers should be strain gauges, low-frequency accelerometers, and displacement sensors. Analog signal transmission lines are cables that connect primary converters with recording devices with an operating voltage of up to 10 V and are components of the measuring system. Cables must be shielded, resistant to lubricants, have at least six cores, the flexibility of the cable must correspond to class 1 or 2 and not change its properties at temperatures from minus 40 °C to plus 80 °C.

The mobile system should provide the possibility of autonomously conducting control tests of dynamic diagnostics of rolling stock units in order to determine the load of running parts, as the main component of checking the quality of capital repairs, assessing the residual resource of load-bearing structures, performing control tests as part of works to extend the designated service life and determining loads of running parts under conditions of rolling stock operation.

2.4.2 MEASUREMENT INFORMATION COLLECTION SUBSYSTEM

The measurement information collection subsystem collects, stores, and visualizes changes in the information signals of displacement sensors, vibration accelerations, and mechanical deformations. In addition, data from the GPS receiver is used to analyze the influence of movement speed on changes in controlled parameters, receive accurate time signals, and determine current coordinates.

The developed acquisition subsystem provides the operation of a CompactRIO controller with a chassis of 8 modules with a built-in programmable logic devices (PLD) and two universal 9205 ADC modules with a maximum sampling frequency of 250 kHz and five 9237 strain gauge modules with a maximum frequency of 50 kHz per channel, module – GPS signal receiver.

In addition to the collection modules, for time synchronization and acquisition of current speed and coordinates, a GPS receiver is also connected to the controller, which is installed on the chassis in the same way as standard modules. Because the receiver is manufactured by a third-party company, the LabView Real Time Module does not have a standard means of acquiring GPS data, so it uses a set of closed virtual devices that are installed separately to interact with it. In addition, to ensure the correct functioning of the module as part of the project, it is also possible to add the SubVIs supplied with the module to the FPGA VI. If the initialization is successful, the GPS data is presented as a cluster or directly in a text format that can be used to debug the software or perform other tasks [37].

2.4.3 SYSTEM FOR DETERMINING MOVEMENT SMOOTHNESS

The subsystem for determining movement smoothness is based on the requirements of the standard on requirements for the movement smoothness of railway rolling stock [29]. The specified standard is intended to check the conformity of the smoothness indicator of the car W_z with the

norms stipulated in the technical documentation for the cars. The smoothness indicator depends on the intensity and spectral composition of the accelerations of the car body.

According to the accepted methodology, the indicators of the movement smoothness W_z are calculated from the acceleration of the body over the pivot nodes at the output of the "physiological filter". According to this, smoothness indicators are calculated in the vertical (W_{zv}) and horizontal (W_{zh}) directions. Data in **Table 2.2** characterize the assessment of movement smoothness.

Table 2.2 Evaluation of the car's running qualities based on the W_z movement smoothness indicator

Parameter	Value, m/s²
Perfectly	2
Good	2–2.5
Sufficient for passenger cars	2.5–3
Limit for passenger cars	3–3.25
Sufficient for freight cars	3.6–4
Limit for freight cars	4–4.25
Limit for a person from a physiological point of view	4.5
Dangerous from the point of view of derailment of rolling stock	5

The calculation of movement smoothness indicators is implemented according to the following algorithm: the size of the block for calculations is determined; the size of the input block is determined by the logarithm to the base two, and with the help of the built-in function of LABVIEW, the Fourier transform is performed to construct the power spectrum; on the basis of the Fourier transformation, frequency arrays and data arrays are formed in the specified frequency range from 0.5 Hz to 20 Hz; the value of the normalized amplitude-frequency characteristic of the correcting filter is calculated.

The final movement smoothness indicator W_z for the data array is calculated according to the formula [29]:

$$W_j = \alpha \cdot \tilde{a}_{kJ}^{0.3}, \tag{2.10}$$

where $\tilde{a}_{kJ}^{0.3}$ – the average square value of vibration accelerations at the output of the correcting filter, m/s²; $\alpha = 4.346$ for vertical oscillations; $\alpha = 4.676$ for horizontal (transverse) oscillations.

An example of the results of the assessment of the movement smoothness is shown in **Fig. 2.21**. It is possible to compare the obtained values of movement smoothness indicators with the permissible limit value $[W_z] = 3.75$.

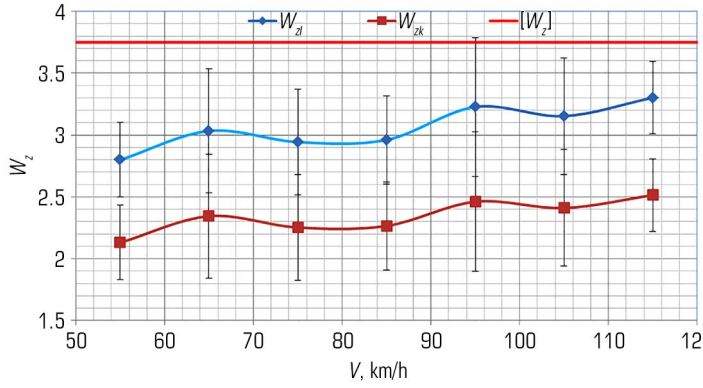

Fig. 2.21 Indicators of movement smoothness in the vertical direction: W_{zl} – indicator of movement smoothness in the pivot section; W_{zk} – indicator of movement smoothness in the car body

2.4.4 SYSTEM FOR DETERMINING TRAFFIC SAFETY INDICATORS

The subsystem for determining security indicators is designed to work in the express processing mode. This subsystem is a set of software installed on a PC and realizes the determination and display of safety indicators in real time with the interval of updating the result once every two seconds or once every 100 meters of the traveled path.

According to the current methods of field tests on railways with a gauge of 1520 mm, it is envisaged to determine traffic safety indicators based on the so-called "frame forces" that act on the wheel pairs from the frame structures of the running parts. However, due to the fact that these characteristics do not give a direct picture of the force interaction of the wheels with the rails, this leads to a decrease in the reliability of the results obtained in the process of running studies.

On the railways of the EU countries, the assessment of safety indicators of the movement of high-speed rolling stock is regulated by standards that establish the following test methods:

– normal method: measurement of contact interaction forces in the horizontal transverse (Y) and vertical (Q) directions;

– simplified method: measurement of lateral force (H) and body accelerations in transverse $\left(\ddot{y}^*\right)$ and vertical $\left(\ddot{z}^*\right)$ directions;

– simplified method: measurement of lateral accelerations of the cart frame $\left(\ddot{y}^+\right)$ and body accelerations in the transverse $\left(\ddot{y}^*\right)$ and vertical $\left(\ddot{z}^*\right)$ directions.

In order to introduce modern approaches to the evaluation of traffic safety indicators, work was carried out on the technical implementation of a simplified test method based on the measurement of accelerations $\left(\ddot{y}^+, \ddot{y}^*, \ddot{z}^*\right)$.

After filtering, the mathematical expectation (x) and standard deviation (s) are calculated to further determine the maximum possible acceleration values (X_{max}) according to the following formula:

$$X_{max} = \bar{x} + k \cdot s, \tag{2.11}$$

where k – coefficient that depends on the given confidence level (to determine the security indicators $k=3$).

The values determined in this way are compared with the maximum permissible values specified by the UIC 518 standard as follows: for vertical accelerations of the body $\left(\ddot{z}_s^*\right)_{lim} = 3$ m/s^2; for lateral accelerations of the body – $\left(\ddot{y}_s^*\right)_{lim} = 3$ m/s^2 when moving straight and in curves with a large radius; $\left(\ddot{y}_s^*\right)_{lim} = 2.8$ m/s^2 – in curves with a radius of $400 \le R \le 600$ m; $\left(\ddot{y}_s^*\right)_{lim} = 2.6$ m/s^2 – in curves with a radius of $250 \le R \le 400$ m. For transverse accelerations of the cart frame, the maximum permissible accelerations are determined as follows:

$$\left(\left(\ddot{y}_s^+\right)_{lim}\right)_{lim} = 12 - M_b/5, \tag{2.12}$$

where M_b – the cart mass in tons.

Experimental implementation of the subsystem was carried out on the basis of the results of road tests.

Fig. 2.22 presents the root-mean-square deviations of the horizontal transverse accelerations of the cart frame recorded during the movement of the experimental train. Based on the fact that the mass of the cart is 6.68 tons, the value $\left(\ddot{y}_s^+\right)_{lim} = 5.33$ m/s^2.

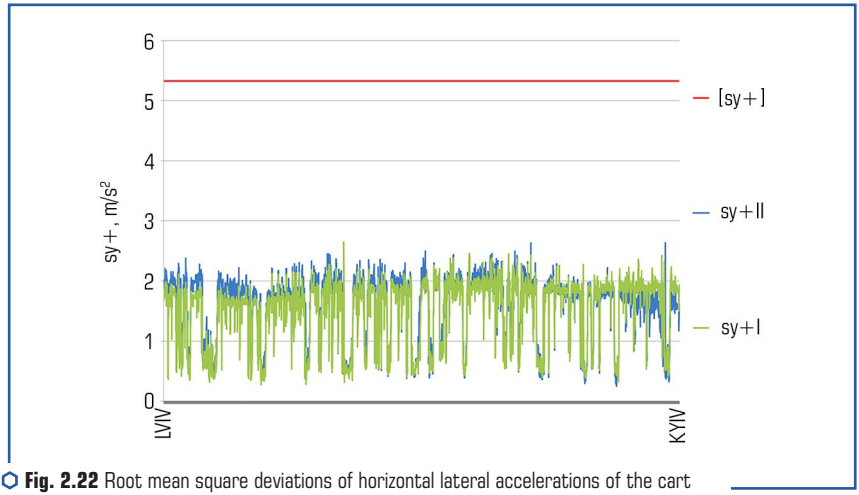

Fig. 2.22 Root mean square deviations of horizontal lateral accelerations of the cart frame measured during the test road

As can be seen from the presented results, the largest rms deviations of accelerations are at least two times lower than the maximum permissible value, which indicates a significant margin of stability of the car from derailment.

CONCLUSIONS

Subsection 2.1 offers three methods and approaches for assessing quality indicators, traffic safety and technical condition of railway rolling stock. The method of measuring mechanical stresses in the surface layers of the elements of the load-bearing structures of the rolling stock by the tensometry method makes it possible to assess the indicators of the technical condition and safety of the movement of the railway rolling stock in its defined dangerous zones. For example, this method allows to determine the vertical and horizontal transverse (frame) forces acting on wheel pairs, according to the rules that are currently in force on railways with a gauge of 1520 mm. The method of measuring contact forces: due to the deformation of the discs of the wheels of the wheel pairs. The proposed method of measuring contact forces makes it possible to directly measure contact forces, thereby evaluating the real traffic safety indicators for this experimental rolling stock, in contrast to the existing method: measurement by deformations of cart frames, which gives only an indirect assessment and does not apply to the conditions of passenger train traffic above 140 km/h.

In subsection 2.2, a method of in-depth processing of the results of road tests of rolling stock is proposed. The essence is to perform a spectral analysis of dynamic processes for various elements of the load-bearing structures of the freight car, with the aim of identifying the relationships between the oscillatory processes of the load-bearing structures and the frequencies at which the interaction between them occurs. A software algorithm for in-depth assessment of experimental indicators of the quality of the movement of freight cars with reduced containers is developed.

In subsection 2.3, the general requirements for the mobile system for determining the quality and safety indicators of the movement of freight cars with reduced containers in operation are formed and implemented. This mobile system allows running tests without involving the laboratory car, which reduces costs and time for conducting such tests by 25.8 %. Based on the results of the practical research, it is established that a decrease in the tare mass index by more than 10 % negatively affects the quality indicators of the movement of such cars, and a speed range of 60–70 km/h was found, during which a sharp deterioration of the movement dynamics indicators was recorded in a number of experimental cars. A safe scheme for the formation of trains, which include freight cars with reduced containers, is proposed. The compression force values obtained during running dynamic tests, which act on autocoupling devices of cars and reach or exceed critical values in the main and middle parts of the train according to the following schemes. It is advisable to place empty cars in the last third of the train.

In subsection 2.4, the general requirements for the software and hardware complex for determining the dynamic load of running parts in the conditions of operation of the rolling stock are

formulated. Technical solutions are implemented regarding the means of running tests of rolling stock to determine the dynamic loading of running parts in operating conditions, which increases the effectiveness of forecasted assessments and increases the efficiency of testing. A set of software subsystems for collecting measurement information, determining movement smoothness and safety indicators of rolling stock according to simplified schemes is developed.

REFERENCES

1. Novachuk, Y., Koblov, R., Teplyakov, A., Egorov, P. (2016). Innovative Method of Determination of Speed of Interaction of Wheels with Rails. Procedia Engineering, 165, 1503–1511. https://doi.org/10.1016/j.proeng.2016.11.886
2. Xu, L., Chen, X., Li, X., He, X. (2018). Development of a railway wagon-track interaction model: Case studies on excited tracks. Mechanical Systems and Signal Processing, 100, 877–898. https://doi.org/10.1016/j.ymssp.2017.08.008
3. Rakshit, U., Malakar, B., Roy, B. K. (2018). Study on Longitudinal Forces of a Freight Train for Different Types of Wagon Connectors. IFAC-PapersOnLine, 51 (1), 283–288. https://doi.org/10.1016/j.ifacol.2018.05.074
4. Lai, J., Xu, J., Wang, P., Yan, Z., Wang, S., Chen, R., Sun, J. (2021). Numerical investigation of dynamic derailment behavior of railway vehicle when passing through a turnout. Engineering Failure Analysis, 121, 105132. https://doi.org/10.1016/j.engfailanal.2020.105132
5. Clarhaut, J., Hayat, S., Conrard, B., Coquempot, V. (2010). The concept of the smart wagon for improving the safety of a railroad transportation system. IFAC Proceedings Volumes, 43 (8), 638–643. https://doi.org/10.3182/20100712-3-fr-2020.00102
6. Lai, J., Xu, J., Liao, T., Zheng, Z., Chen, R., Wang, P. (2022). Investigation on train dynamic derailment in railway turnouts caused by track failure. Engineering Failure Analysis, 134, 106050. https://doi.org/10.1016/j.engfailanal.2022.106050
7. Rezvani, M. A., Mazraeh, A. (2017). Dynamics and stability analysis of a freight wagon subjective to the railway track and wheelset operational conditions. European Journal of Mechanics – A/Solids, 61, 22–34. https://doi.org/10.1016/j.euromechsol.2016.08.011
8. Wu, B., Xiao, G., An, B., Wu, T., Shen, Q. (2022). Numerical study of wheel/rail dynamic interactions for high-speed rail vehicles under low adhesion conditions during traction. Engineering Failure Analysis, 137, 106266. https://doi.org/10.1016/j.engfailanal.2022.106266
9. Fomin, O., Lovska, A., Píštěk, V., Kučera, P. (2019). Dynamic load computational modelling of containers placed on a flat wagon at railroad ferry transportation. Vibroengineering Procedia, 29, 118–123. https://doi.org/10.21595/vp.2019.21132
10. Khan, M. R., Dasaka, S. M. (2018). Wheel-rail Interactions in High Speed Railway Networks during Rapid Train Transit. Materials Today: Proceedings, 5 (11), 25450–25457. https://doi.org/10.1016/j.matpr.2018.10.350

11. Xu, L., Zhai, W. (2019). A three-dimensional model for train-track-bridge dynamic interactions with hypothesis of wheel-rail rigid contact. Mechanical Systems and Signal Processing, 132, 471–489. https://doi.org/10.1016/j.ymssp.2019.04.025
12. Sun, Y. Q., Dhanasekar, M. (2002). A dynamic model for the vertical interaction of the rail track and wagon system. International Journal of Solids and Structures, 39 (5), 1337–1359. https://doi.org/10.1016/s0020-7683(01)00224-4
13. Xia, F., Cole, C., Wolfs, P. (2008). The dynamic wheel-rail contact stresses for wagon on various tracks. Wear, 265 (9-10), 1549–1555. https://doi.org/10.1016/j.wear.2008.01.035
14. Okorokov, A., Fomin, O., Lovska, A., Vernigora, R., Zhuravel, I., Fomin, V. (2018). Research into a possibility to prolong the time of operation of universal open top wagon bodies that have exhausted their standard resource. Eastern-European Journal of Enterprise Technologies, 3 (7 (93)), 20–26. https://doi.org/10.15587/1729-4061.2018.131309
15. Gorobchenko, O., Fomin, O., Gritsuk, I., Saravas, V., Grytsuk, Y., Bulgakov, M. et al. (2018). Intelligent Locomotive Decision Support System Structure Development and Operation Quality Assessment. 2018 IEEE 3rd International Conference on Intelligent Energy and Power Systems (IEPS). Kharkiv, 239–243. https://doi.org/10.1109/ieps.2018.8559487
16. Fomin, O., Sulym, A., Kulbovskyi, I., Khozia, P., Ishchenko, V. (2018). Determining rational parameters of the capacitive energy storage system for the underground railway rolling stock. Eastern-European Journal of Enterprise Technologies, 2 (1 (92)), 63–71. https://doi.org/10.15587/1729-4061.2018.126080
17. Sulym, A. O., Fomin, O. V., Khozia, P. O., Mastepan, A. G. (2018). Theoretical and practical determination of parameters of on-board capacitive energy storage of the rolling stock. Naukovyi Visnyk Natsionalnoho Hirnychoho Universytetu, 5, 79–87. https://doi.org/10.29202/nvngu/2018-5/8
18. Gorbunov, M. I., Fomin, O. V., Prosvirova, O. V., Prokopenko, P. M. (2019). Conceptual basis of thermo-controllability in railway braking tribo pairs. Naukovyi Visnyk Natsionalnoho Hirnychoho Universytetu, 2, 58–66. https://doi.org/10.29202/nvngu/2019-2/5
19. Fomin, O., Lovska, A., Radkevych, V., Horban, A., Skliarenko, I., Gurenkova, O. (2019). The dynamic loading analysis of containers placed on a flat wagon during shunting collisions. ARPN Journal of Engineering and Applied Sciences, 14 (21), 3747–3752. Available at: http://www.arpnjournals.org/jeas/research_papers/rp_2019/jeas_1119_7989.pdf
20. Marye, G. (1933). Vzaimodeistvie puti i podvizhnogo sostava. Moscow: Goszheldorizdat, 338.
21. Nadal, M. (1908). Locomotives a Vapeur Collection Encyclopedia Scintifique Biblioteque de Mecanique Applique et Genie, Paris,186.
22. Mishchenko, K. (1950). Sovremennoe sostoianie voprosa o vspolzanii kolesa na rels. Trudy DIIT, XX, 53–67.
23. Sapronova, S., Tkachenko, V., Fomin, O., Hatchenko, V., Maliuk, S. (2017). Research on the safety factor against derailment of railway vehicless. Eastern-European Journal of Enterprise Technologies, 6 (7 (90)), 19–25. https://doi.org/10.15587/1729-4061.2017.116194

24. Krol, O., Sokolov, V. (2020). Research of toothed belt transmission with arched teeth. Diagnostyka, 21 (4), 15–22. https://doi.org/10.29354/diag/127193
25. Melnyk, O., Onishchenko, O., Onyshchenko, S., Golikov, V., Sapiha, V., Shcherbina, O., Andrievska, V. (2022). Study of Environmental Efficiency of Ship Operation in Terms of Freight Transportation Effectiveness Provision. TransNav, the International Journal on Marine Navigation and Safety of Sea Transportation, 16 (4), 723–729. https://doi.org/10.12716/1001.16.04.14
26. Melnyk, O., Onyshchenko, S., Onishchenko, O., Shumylo, O., Voloshyn, A., Koskina, Y., Volianska, Y. (2022). Review of Ship Information Security Risks and Safety of Maritime Transportation Issues. TransNav, the International Journal on Marine Navigation and Safety of Sea Transportation, 16 (4), 717–722. https://doi.org/10.12716/1001.16.04.13
27. Masliev, V. (2002) Dinamika lokomotiva s ustroistvom dlia radialnoi ustanovki kolesnykh par v krivykh. Visnyk Skhidnoukr. nats. un-tu. Tekhnichni nauky. Seriia Transport., 6 (52), 69–74.
28. Sagin, S., Kuropyatnyk, O., Sagin, A., Tkachenko, I., Fomin, O., Píštěk, V., Kučera, P. (2022). Ensuring the Environmental Friendliness of Drillships during Their Operation in Special Ecological Regions of Northern Europe. Journal of Marine Science and Engineering, 10 (9), 1331. https://doi.org/10.3390/jmse10091331
29. SOU MPP 45.060-204:2007. Vahony pasazhyrski. Plavnist rukhu. Metody vyznachennia (2007). Kyiv: Minprompolityky Ukrainy, 12.
30. Kondratiev, A., Slivinsky, M. (2018). Method for determining the thickness of a binder layer at its non-uniform mass transfer inside the channel of a honeycomb filler made from polymeric paper. Eastern-European Journal of Enterprise Technologies, 6 (5 (96)), 42–48. https://doi.org/10.15587/1729-4061.2018.150387
31. Kondratiev, A. (2019). Improving the mass efficiency of a composite launch vehicle head fairing with a sandwich structure. Eastern-European Journal of Enterprise Technologies, 6 (7 (102)), 6–18. https://doi.org/10.15587/1729-4061.2019.184551
32. Pogorelov, D., Simonov, V. (2010). An indicator for assessing the danger of rolling stock derailing by rolling a wheel onto the rail head. Newsletter of the Eastern Ukrainian National University named after V. Dahl, 5 (147), I, 64–70.
33. Dyomin, Yu. V., Chernyak, G. Yu. (2003). Osnovy dynamiky vahoniv. Kyiv: KUETT, 270.
34. Chernyak, A. Yu., Diomin, Yu. V., Zakhovaiko, O. P., Shevchuk, P. A. (2014). Computer modeling of the dynamics of rack transport vehicles. News of the National News. tech. University of Ukraine "Kiev Polytechnic Institute". Machine-building series, 94–98.
35. Chernyak, A. Yu. (2009). Primenenie kompiuternogo modelirovaniia dlia opredeleniia veroiatnykh prichin skhoda s relsov gruzovykh vagonov. Zaliznichnii transport Ukraini, 3, 49–52.
36. Chernyak, A. Yu. (2010). Computer model for prompt determination of the probable causes of derailment of freight cars. News of Skhidnoukrain National University im. V. Dahl, 5 (147), 1, 40–46.
37. Samsonkin, V. M., Chernyak, G. Yu. (2012). Before assessing the risks of building a dry warehouse from slats on a computer modeling stand, Zalizny Transport Ukraine, 2, 39–42.